

Aberration-free high-bandwidth holographic imaging

Zhengzhong Huang, Liangcai Cao*

State Key Laboratory of Precision Measurement Technology and Instruments, Department of Precision Instruments, Tsinghua University, Beijing 100084, China;

* clc@tsinghua.edu.cn

ABSTRACT

Objective measurements of the morphology and dynamics of label-free cells and tissues can be achieved by quantitative phase with low phototoxicity and no photobleaching. Modern quantitative optical imaging possesses a huge information capacity. The morphology and dynamics of label-free tissues can be exploited by sample-induced changes in the optical field from quantitative phase imaging. Its sensitivity to subtle changes in the optical field makes the reconstructed phase susceptible to phase aberrations. We present aberration-free high-bandwidth holographic microscopy which exploits high-throughput label-free quantitative phase imaging. Firstly, a full-bandwidth holographic reconstruction is retrieved from interferograms by establishing a holographic multiplexing framework. Based on the analyticity of band-limited signal under a diffraction-limited system, the maximum space bandwidth utilization limit in a single multiplexing hologram is increased to the maximum sensor limit. Secondly, A variable sparse splitting framework on quantitative phase aberration extraction is imported based on the alternating direction aberration-free method. By formulating the aberration extraction as a convex quadratic problem, the background phase aberration can be fast and directly decomposed with the specific complete basis functions such as Zernike or standard polynomials. Faithful high throughput phase reconstruction can be obtained by eliminating global background aberration. It opens a new route to multiplexing quantitative optical imaging and helps to improve the performance of constraint-free modern optical microscopes in various spectral regimes.

Keywords: High bandwidth; Aberration; Phase.

1. INTRODUCTION

Accurate detection of spatial and temporal wave propagation is essential for the study of the interaction between objects and waves. Digital holography records the entire complex wavefront by introducing the reference wave [1, 2], becoming a powerful technique of quantitative phase imaging (QPI). Modern quantitative optical imaging is developing toward high throughput and powerful data processing capabilities [3]. Off-axis holography can achieve separation of the object wave and conjugate wave by introducing a tilted reference wave. Limited bandwidth of the object wave is usually required in microscopy under coherent illumination, which may limit the resolution or field of view (FOV) and space bandwidth product (SBP).

The optical aberration limits the ability to observe structures at diffraction-limited resolutions, which causes inconsistencies between images obtained from different setups [4]. Optical aberration in holographic imaging depends on the sample or sample holders because of the mismatch in refractive index between optical elements and inaccurate estimation of the reference wave [5, 6]. The use of microscopic objective (MO) introduces phase aberrations that can be superposed over the biological sample. A successful image reconstruction theoretically requires tedious alignment and precise measurement of the system parameters. The sensitivity of quantitative phase reconstruction to subtle changes in the optical field makes the phase reconstruction susceptible to optical aberrations. These phase aberrations may severely hinder the quantitative measurement of the object's thickness or height with distorted visualization [7].

In this letter, we introduce a high-bandwidth holographic multiplexing framework. A high bandwidth holographic microscope (HBHM) was built based on the framework, enabling an 8-fold space-bandwidth product (SBP) enhancement with conventional off-axis interference for the same camera [8]. Its sensitivity to subtle changes in the optical field makes the reconstructed phase susceptible to phase aberrations. We introduce a phase variable splitting framework based on alternating direction sparse optimization for background aberration extraction [9, 10]. Faithful phase reconstruction can be obtained, relaxing the strict alignment requirements for tolerating system aberrations.

2. METHODS

2.1 Title

Figure 1(a) shows the optical configuration of HBHM. The framework of the configuration is built based on the Mach–Zehnder interferometer, which comprises three major components: a light source, a transmission microscope system, and a multiplexing system. The transmission microscopic system includes a microscope objective (MO) with a tube lens (TL). In the multiplexing interferometric module, Lens (L) 1 and L2 were positioned in a $4f$ system. The focal length of L1 and L2 could be adjusted as needed to increase its spatial spectrum occupancy. The image output from the microscope system was optically Fourier transformed by L1 while being split into two beams using BS2 to form two independent sample channels. Two images of different FOVs are projected in the sensor with different directions of chief ray propagation. The relationship between the object waves and the reference wave is shown in Fig. 1(b). The sample $S_1(\mathbf{r})$ and $S_2(\mathbf{r})$ are multiplexed by using a reference quasi-plane wave [8]:

$$I(\mathbf{r}) = |R(\mathbf{r}) + S_1(\mathbf{r}) + S_2(\mathbf{r})|^2. \quad (1)$$

The emergent sample waves are modulated by the optical coherent transfer function of the imaging system. The spatial frequency distribution of the hologram is shown in Fig. 1(c). The shape of the sample's spectrum is generally circular, and its radius is determined by the objective numerical aperture (NA) and magnification. In the high bandwidth holographic multiplexing framework, the sample's function needs to meet two conditions: First, the sample wave is bandwidth-limited. Second, each complete spectrum of the sample is moved to the positive half-axis of the spectrum by introducing a reference wave. $I(\mathbf{r})/R(\mathbf{r})$ is operated by logarithmic transformation and $\text{Re}[H(\mathbf{r})] = 0.5 \ln I(\mathbf{r})/|R(\mathbf{r})|^2$ is obtained. The directional Hilbert transform is identical to obtaining the complex-amplitude of samples [11]:

$$\text{Im}[H(\tau)] = i\mathcal{F}^{-1} \left\{ \mathcal{F} \left\{ \text{Re}[H(\mathbf{r})] \right\} \text{sgn}(\mathbf{k} \cdot \mathbf{k}_{\parallel}) \right\}, \quad (2)$$

where ‘sgn’ is the signum-function, and \mathcal{F} is the two-dimensional Fourier transform, and $\mathbf{k} = k_{\parallel}\mathbf{k}_{\parallel} + k_{\perp}\mathbf{k}_{\perp}$ represents the coordinates in the Fourier domain. As shown in Fig. 1(c), the object waves are distributed along the coordinates \mathbf{k}_{\parallel} . Then the complex-amplitude of the object wave can be reconstructed. By comparing with the conventional off-axis interferogram with bandwidth $B_o = 0.25B_c$, the size of the Fourier spectrum of a single complex-wave from the proposed system is 4-fold larger than the conventional one. An 8-fold of the Fourier spectrum area in both two complex-waves can be promoted. The SBP of the proposed system is an 8-fold enhancement by the conventional DHM. The unwrapped phase of reconstruction could be written in this form as $\varphi(\mathbf{r}) = \varphi_s(\mathbf{r}) + \varphi_a(\mathbf{r})$, where $\varphi_s(\mathbf{r})$ is the sample phase, $\varphi_a(\mathbf{r})$ is the background aberration introduced by the optical elements. Figure 1(d) shows the directly reconstructed phase with background phase aberration. The base of the aberration can be defined by Zernike polynomials

$$\varphi_{az}(\mathbf{r}) = -\sum_{\gamma=0}^n P_{\gamma} Z_{\gamma}(\mathbf{r}), \quad (3)$$

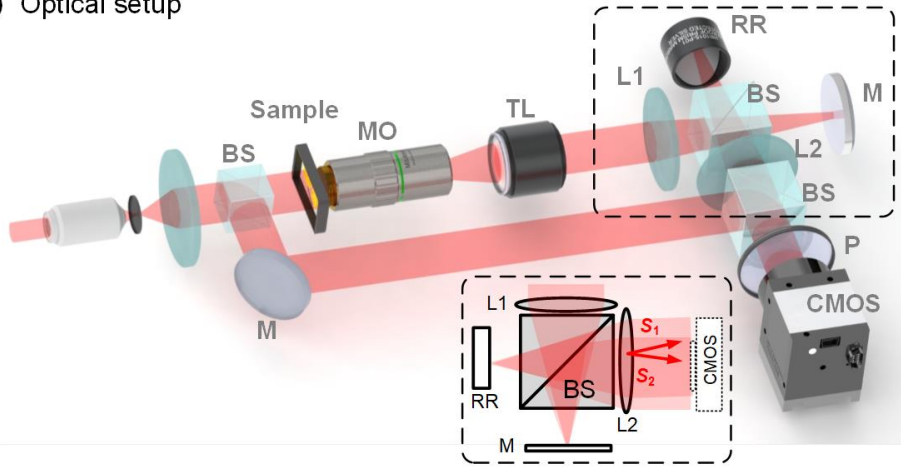
where P_{γ} is the coefficient of each order in Zernike polynomials, respectively. Z_{γ} is the γ th order Zernike polynomial. The aberration measurement can be modeled as a linear combination of the Zernike coefficients and polynomials. Optical aberration in holographic imaging depends on the sample or sample holders due to the mismatch in refractive index (RI) between optical elements in the imaging system and inaccurate estimation of the reference wave [5]. The background phase aberration can be decomposed with the Zernike polynomials, which are a better choice in the lens-based imaging system. The total reconstructed phase can be separated by target object and background aberration, and they can be solved by a minimization problem:

$$\min \|\mathbf{b} - \mathbf{o} - \mathbf{A}\mathbf{p}\|_2^2 + f(\mathbf{v}) + g(\mathbf{o}),$$

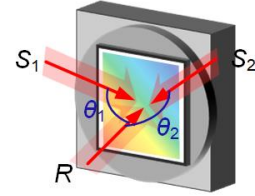
$$\text{s.t. } \mathbf{v} = \mathbf{p}, \mathbf{A}\mathbf{p} + \mathbf{o} = \mathbf{b},$$
(4)

where \mathbf{b} is the total phase reconstruction, \mathbf{o} is assumed as the sample distribution, \mathbf{A} is the matrix of the Zernike polynomial base. \mathbf{v} is the Zernike coefficient in each polynomial. The $f(\mathbf{v})$ and $g(\mathbf{o})$ are objective functions with $f(\mathbf{v}) = \mu_1 \|\mathbf{v}\|_1$ and $g(\mathbf{o}) = \mu_2 \|\mathbf{o}\|_1$, where μ_1 and μ_2 are parameters. The minimization problem is calculated by the alternating direction method [9, 10]. Figures 1(e) and 1(f) show the object and the background aberration, respectively. The coefficient of Zernike polynomials can be calculated quantitatively.

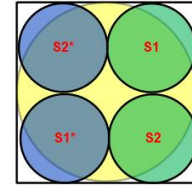
(a) Optical setup



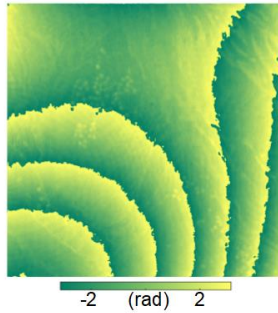
(b) Recording



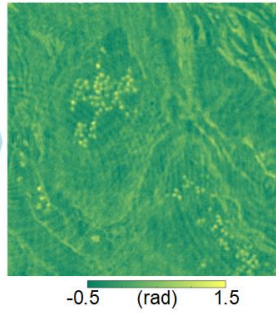
(c) Maximum



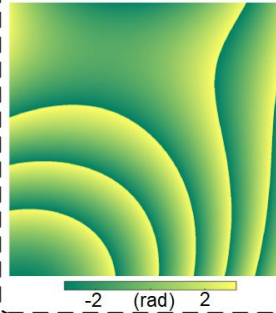
(d) Phase



(e) Aberration-free



(f) Aberration



Coefficient

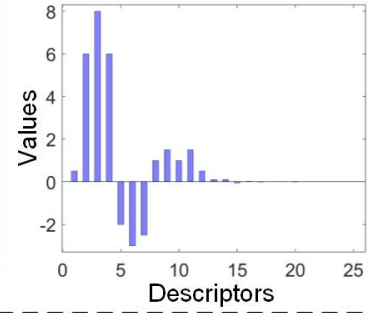


Fig 1. (a) The optical setup of high bandwidth holographic system. RR: Retro-reflector, BS: Beam splitter. (b) The relationship between the object waves and the reference wave. (c) The spatial frequency spectrum of the hologram from the high bandwidth holographic system. (d) Reconstructed phase. (e) The phase after phase elimination. (f) The final reconstructed aberration from (e) and the coefficients in each descriptor of the first 15 Zernike basis polynomials.

3. RESULTS

Figures 2(a) shows the Fourier space of the detection from the proposed HBHM. The spatial frequency spectrum shows similar features to Fig. 1(c). After aberration compensation based on the Zernike polynomials, Figure 2(b) shows the reconstructed aberration-free phase by using HBHM. The magnification of the MO is 20 \times with 0.42 NA. The 4f system by using L1 and L2 is 1 \times magnification and the total magnification of 20 \times . The whole motivation of the background elimination is to ensure proper object phase visualization. A flat phase in the background is crucial for correct analysis. For comparison, Figure 2(c) shows the Fourier space of the detection from the conventional off-axis DHM. The 4f

system by using L1 and L2 is $2\times$ magnification and the total magnification of $40\times$. So the radius of the object's bandwidth is half of the case in Fig. 2(a). Figure 2(d) shows the reconstructed phase of conventional off-axis DHM. The area of the object wave is smaller than the proposed HBHM. In the HBHM, the reconstruction doubles the camera's FOV and shows 8-fold SBP enhancement with conventional off-axis holographic imaging.

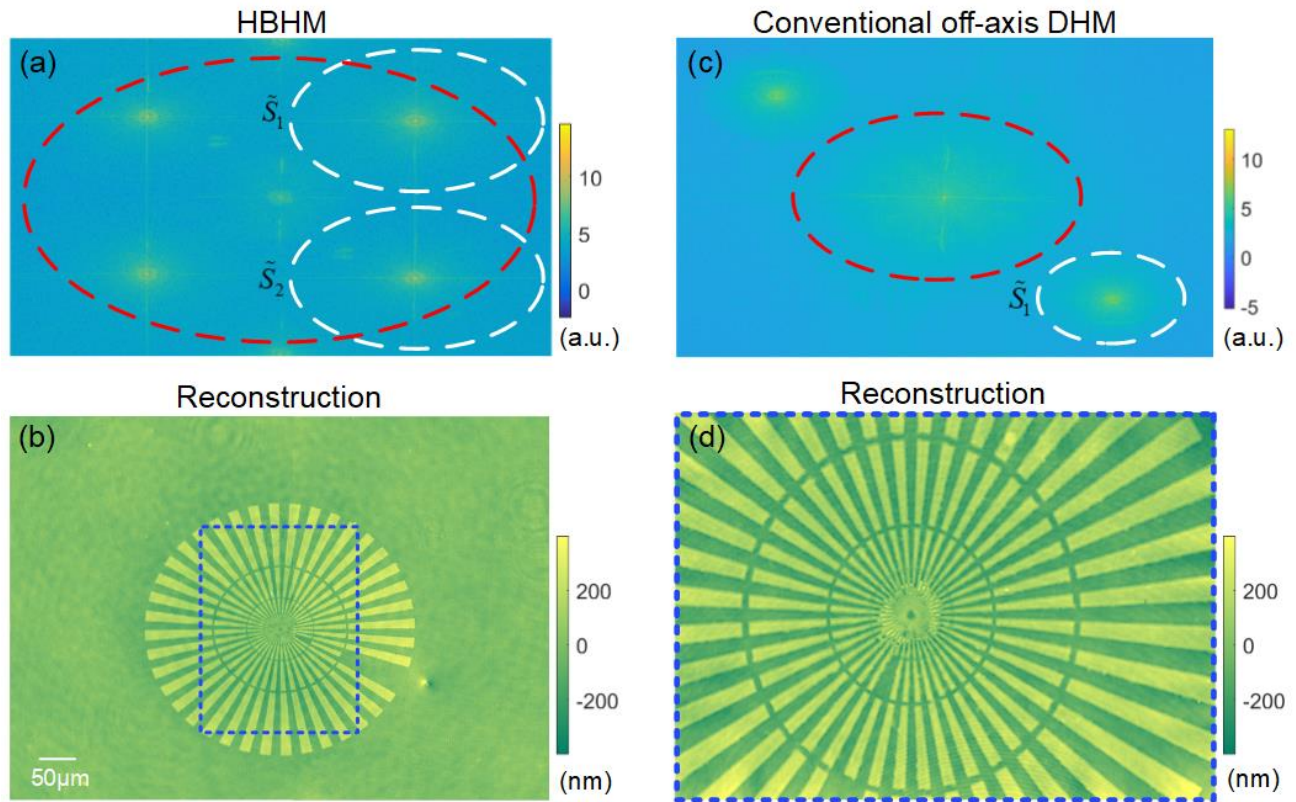


Fig. 2. (a) The Fourier space of the detection from the proposed HBHM. (b) The reconstructed phase of the phase ring target from the proposed HBHM. (c) The Fourier space of the detection from the conventional off-axis DHM. (d) The reconstructed phase of conventional off-axis DHM.

Figure 3(a) shows the label-free tissue on glass slide. The sample was a formalin-fixed paraffin-embedded tissue block from a normal intestinal endocrine tumor. The tissue block was cut into $4\ \mu\text{m}$ thick and it was finally repackaged with permount. The red box in the slide is the area of the tissue and its corresponding shape with hematoxylin and eosin (H&E) stained. Figure 3(b) shows the direct reconstruction from the proposed HBHM. Figure 3(c) shows the pseudo-3D view of reconstructed aberration by using the proposed method based on the Zernike polynomials from the 1st term to the 15th term. Figure 3(d) shows the corresponding coefficients of these Zernike polynomials. After using a conjugated phase compensation, the reconstructed phase shows a clear cell characteristic, as shown in Fig. 3(e). The fitting model to higher order is expanded straightforwardly for more complex aberrations if high-order aberrations in the experiment must be removed. The motivation of the aberration elimination is to ensure proper cell phase for further analysis without a phase offset error.

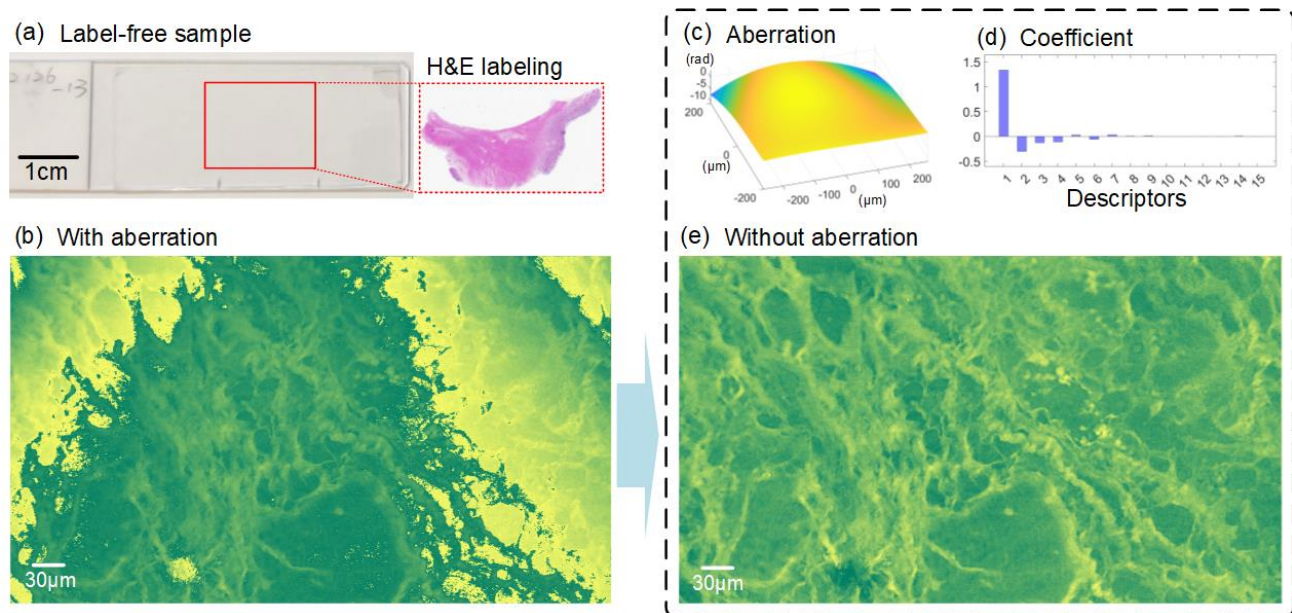


Fig. 3. (a) The label-free normal colonic mucosa. (b) The reconstructed phase from the proposed system. (c) The final reconstructed aberration from (b). (d) The Zernike coefficients in each descriptor of the first 15 Zernike basis polynomials. (e) The phase after aberration compensation.

4. DISCUSSION

Interpretation of phase provides highly sensitive measurements for studying biological physiological processes and material characterizing. We demonstrated HBHM based on high bandwidth holographic multiplexing framework, which enables an 8-fold SBP enhancement with conventional off-axis reconstruction for the same camera. It efficiently utilized the interferogram bandwidth of the intensity matrix. Wide FOV and high bandwidth reconstruction can be achieved without compromising either the space bandwidth or the acquisition rate. To achieve aberration-free phase reconstruction, A phase variable splitting framework for background aberration extraction is introduced based on the alternating direction method. An accurate background aberration can be separated from the direct reconstructed phase by imposing the sparsity regularization on the object and the coefficients of bases. It may serve as a vital tool to explore the function of overall label-free tissue and cells. We expect that it empowers applications in high-throughput, large-scale studies of label-free pathology.

REFERENCES

1. Goodman, J. W. Introduction to Fourier optics (Roberts & Company Publishers, 2005), 3rd ed.
2. Huang, Z. Z., Memmolo, P., Ferraro, P. and Cao, L. C. "Dual-plane coupled phase retrieval for non-prior holographic imaging," *Photonix*. **3**, 3 (2022).
3. Park, J., Brady, D., Zheng, G., Tian, L. and Gao, L. "Review of bio-optical imaging systems with a high space-bandwidth product," *Adv. Photonics*. **3**: 044001 (2021).
4. Booth, M. J. "Adaptive optical microscopy: the ongoing quest for a perfect image," *Light Sci. Appl.* **3**, e165 (2014).
5. Meier, R. W. "Magnification and third-order aberrations in holography," *J. Opt. Soc. Am.* **55**, 987 (1965).
6. Wyant, J. C. and Creath, K. Basic wavefront aberration theory for optical metrology, applied optics and optical engineering, Vol. XI, Chap. 1, (Academic Press, Boston, MA, 1992).

7. Sirico, D. G., Miccio, L., Wang, Z., Memmolo, P., Xiao, W., Che, L. P., Xin, L., Pan, F. and Ferraro, P. "Compensation of aberrations in holographic microscopes: main strategies and applications," *Appl. Phys. B.* 128, 78 (2022).
8. Huang, Z. Z. and Cao, L. C. "High Bandwidth-Utilization Digital Holographic Multiplexing: An Approach Using Kramers–Kronig Relations," *Adv. Photonics Res.* 3, 2100273 (2022).
9. Huang, Z. Z., Yang, F., Liu, B., Liu, Y. and Cao, L. C. "Aberration-free synthetic aperture phase microscopy based on alternating direction method," *Opt. Lasers. Eng.* 160. 107301 (2023).
10. Huang, Z. Z. and Cao, L. C. "Phase aberration separation for holographic microscopy by alternating direction sparse optimization," *Opt. Express* 31, 12520-12533 (2023).
11. Titchmarsh, E. C. *Introduction to the theory of Fourier integrals* (Chelsea, New York, 1986).